Hindawi
Advances in Materials Science and Engineering
Volume 2020, Article ID 5687951, 12 pages
https://doi.org/10.1155/2020/5687951

Research Article

Calculation and Estimation of Surface Roughness and Energy Consumption in Milling of 6061 Alloy

Burak Öztürk[1] **and Fuat Kara**[2]

[1]*Metallurgy and Materials Engineering, Bilecik Seyh Edebali University, Bilecik, Turkey*
[2]*Mechanical and Manufacturing Engineering, Düzce University, Düzce, Turkey*

Correspondence should be addressed to Fuat Kara; fuatkara@duzce.edu.tr

Received 22 November 2019; Accepted 26 February 2020; Published 10 April 2020

Academic Editor: Francesco Ruffino

The best surface quality that can be achieved in manufactured products has become the main goal of industrial enterprises in recent years. Due to the subsequent increase in energy consumption costs from rising energy efficiency rates, manufacturers are contributing to this issue by applying advanced design functions for their machines. In line with the same objective, this study investigated the machinability of 6061 aluminum alloy, which has a high throughput rate and low machinability featuring built up edge. The aim of the research was to optimize the cutting parameters for minimum surface roughness (Ra) and energy consumption (EC) using a CNC milling machine. At the same time, measurements of power indices (A) of both the spindle and the *X*-axis motors were carried out with the goal of improved chip removal as compared to literature studies. The experiment was designed according to the Taguchi L_{16} ($2^1 \times 4^3$) orthogonal index. Four different cutting speeds (60, 120, 180, and 240 m/min), feed rates (0.10, 0.15, 0.20, and 0.25 mm/rev), and cutting depths (0.5, 0.10, 0.15, and 0.20 mm) and two different cooling methods (coolant fluid and dry cutting) were selected as cutting parameters.

1. Introduction

Today, energy saving has become a significant consideration in the manufacture of both consumer products and industrial equipment. Studies on energy saving, especially recently, have focused on the required energy consumed in the production sector [1–3] for the manufacture of semi- and fully finished products. The industrial machining process forms an essential part of the global economy. The determination of the optimal criteria for this process can contribute to a maximum number of quality parts being produced at a minimum of energy consumption [4, 5]. Roughness is an important factor in the assessment of mechanical components and can affect their performance. A low roughness value is desirable, but manufacturing costs and difficulties in processing make this a challenging goal. Production costs generally rise in parallel with reduced surface roughness [6]. Energy consumption in the machining process has previously been the subject of many studies. Cutting condition effects on power consumption in the drilling and end milling of S45C carbon steel were determined by Mori et al. using a vertical machining center [7]. In the milling of ASSAB 760 steel performed under dry cutting conditions, Liu et al. measured the forces via a dynamometer and the power consumption by a power meter. As a result, a new machining energy consumption model was introduced [8]. In the turning of AISI 6061 T6, Camposeco-Negrete reported the determination of optimal cutting parameters for minimal surface roughness, cutting force, cutting energy, and energy consumption [9]. Oda et al. experimentally determined the optimal inclined angle for lowering the consumption of energy [10]. In the turning of AISI 1045 steel, Shokoohi et al. determined the impact of the heat generated in the cutting zone on power consumption and workpiece quality [11]. The effects of tool features on power consumption during the processes of drilling and turning were examined by Neugebauer et al. [12]. In addition, Muñoz-Escalona et al. measured the energy

consumption and surface roughness in the end milling of austenitic stainless steel under cryogenic, fluid coolant and dry cutting conditions [13]. Nas and Ozturk applied face milling to a spheroidal graphite cast iron workpiece, measured the increase in the consumed power index (PI) with an ammeter device, and optimized the machining process with two different cutting tools [14].

A model was presented for the establishment of the energy consumption allowance (ECA) according to the movement of the workpiece within the machining system [15]. In the slot milling of Al-7075, a model was proposed for estimating surface roughness. The hybrid technique used to develop the model was a combination of the analytically calculated specific cutting energy consumption (SCEC) and the experimentally characterized correlation of the SCEC and the surface roughness [16].

An examination of the literature studies showed that varying amounts of electrical energy are expended by machine tools depending upon their work loads and environments. During operation, the energy consumption is greater than the energy required to meet the demands of the machine. Consequently, the focus of this study was on the energy consumption throughout the duration of operation [17]. The surface quality of this material is lower than other alloys due to this BUE property. For this reason, it is very important, especially for the automotive and aerospace sectors, for the 6061 series aluminum alloys, which have low processability, to be at their best regarding the surface quality. The energy consumption during cutting (P_{cutting}) gives information about the workability of the material. In this study, the aim was to optimize the cutting parameters to yield minimum surface roughness with minimum energy consumption during the manufacturing process by using the Taguchi method. Energy consumption surveys in the literature do not include measurements for the *X*-axis servo motors, where the cutting force occurs. In this study, the energy consumption values of both the spindle and *X*-axis servo motors during chip removal were examined along with the amount of surface roughness. In addition, the slot milling operation was investigated for the first time under both dry and wet (coolant fluid) cutting conditions.

2. Experimental

2.1. Taguchi Design. In order to achieve a successful outcome when conducting experimental studies, it is essential that the experiments be designed correctly. Thus, the experiments were designed and analyzed via the method of Genichi Taguchi. In this method, results are analyzed using the signal to noise (*S*/*N*) ratio to statistically measure the performance. The evaluation of the experimental results is carried out using the signal factor (*S*) as the actual value from the system and the noise factor (*N*) not as an element of the experimental design, but as an influencing factor on the result. All variables resulting in deviations from the target values for performance characteristics constitute sources of the noise. Dependent upon the quality characteristic, three cases are used when calculating the *S*/*N* ratio: "the nominal is the best," "the largest is the best," and "the smallest is the best" [18, 19]. In the present study, as the lowest values for *Ra* and EC were desired for achieving machining efficiency, the *S*/*N* values were calculated according to "the smallest is best" formula, as expressed in the following equation:

$$\frac{S}{N} = -10\log\left(\frac{1}{n}\sum_{i=1}^{n} y_i^2\right), \tag{1}$$

where y_i represents the surface roughness and energy consumption values and n represents the number of experiments carried out.

The machining parameters were selected as cutting speed (*V*), feed rate (*f*), depth of cut (DOC), and cooling method (Cm). Table 1 presents the control factors and levels applied in the slot milling of the Al T6061 alloy. Table 2 shows the L_{16} orthogonal array utilized in conducting the experiments. In order to determine the variable effect levels on *Ra*, analysis of variance (ANOVA) was applied on the experimental results (CI 95%). Minitab 16 software was used to carry out the experimental design and statistical analysis in accordance with the Taguchi method.

In general, due to their complexity, conventional experimental design approaches are challenging. Moreover, as the number of process parameters is increased, more experimental trials need to be conducted, thus requiring identification and control, under laboratory conditions, of the factors responsible for variations. By using the orthogonal arrays of the Taguchi design technique, the number of experiments can be reduced significantly, and better quality is ensured when the uncontrollable effects of those factors are reduced. Therefore, the Taguchi experimental design and L_{16} orthogonal index given in Table 2 were used for the study.

2.2. Workpiece, Cutting Tools, and Machining Center. In this experimental study, SCC APKT 11T 308-PM series carbide tools, manufactured from TiNN PVD-coated tungsten-cobalt alloy, were used for the processing of the aluminum alloy. Chip removal was carried out by mounting a single insert to the 16 mm diameter APKT 11 R390 holder. The CNC milling machine used in the experiments was the Microcut CNC 1000 model with a 15 KW drive motor (Figure 1(a)). The Microcut vertical machining center has Fanuc spindle drivers. In this study, current transformers were connected to power cables having three phases in the power consumption drive inputs, and the experiments were performed by displaying the measured power index PI (A) from these current transformers using an Entes ammeter (Figure 1(b)).

2.3. Measurement of Energy Consumption and Surface Roughness. Studies in the literature have generally measured changes in spindle servo motor energy consumption during the metal cutting process. Other studies did not consider the fact that energy was consumed with the table axis motor running in the direction of chip removal, whereas this study measured the energy consumed by both the *X*-axis and the spindle axis servo motors simultaneously. By using this

Table 1: Taguchi L_{16} experimental design.

Parameters	Levels			
	Level 1	Level 2	Level 3	Level 4
Cutting speed V (m/min)	60	120	180	240
Feed rate F (mm/rev)	0.1	0.15	0.2	0.25
Depth of cut DOC (mm)	0.5	1	1.5	2
Cooling methods Cm	1 (yes) Wet	2 (no) Dry	—	—

Table 2: Taguchi L_{16} design with orthogonal array.

Exp. no	V (m/min)	f (mm/rev)	a (mm)	Cm
1	1	1	1	1
2	1	2	2	1
3	1	3	3	2
4	1	4	4	2
5	2	1	2	2
6	2	2	1	2
7	2	3	4	1
8	2	4	3	1
9	3	1	3	1
10	3	2	4	1
11	3	3	1	2
12	3	4	2	2
13	4	1	4	2
14	4	2	3	2
15	4	3	2	1
16	4	4	1	1

ammeter, it was possible to measure the energy index with ± 1% accuracy.

The existence of a relationship between the machining power and the electrical current in three-phase motors was suggested by Shokoohi et al. [11]. Equation (2) was used to calculate Ptotal. While two-phase motors work with 220 V, that is, a phase voltage, three-phase motors work with 380 V, that is, three-phase network voltage (in Turkey Network). In the calculation of electrical power equation, besides the power coefficient and voltage, it is the third determining electrical current. In this paper, since other variables are taken as constant, the effect of current change on power change is discussed.

$$P_{\text{total}} = \sqrt{3}.\,\text{V.I.Cos}\,\sigma. \tag{2}$$

In this equation, when the ammeter's current value (I) was measured, the processing voltage value (V) of the CNC vertical machine was 0.38, while the value of the servo motors (Cos σ) was listed in the catalog as 0.6. When calculating the P_{total} value in the chip removal process, the value of the machine during the period when chip is not being removed is defined by different names in the literature, such as (P_{idle}) and (P_{air}). The total power consumption can be used to calculate this value. Equation (3) can be used to calculate the cutting power (P_{cutting}) value, which is the main parameter effective on the surface roughness, tool wear, shear calculation, and chip formation during metal cutting [9, 13, 16].

$$P_{\text{cutting}} = P_{\text{total}} - P_{\text{air}}. \tag{3}$$

Spindle and servo motor energy consumption stems from two sources. The first is the movement of the spindle shaft and workbench and acceleration/deceleration under the influence of inertia, friction resistance, and gravity. The second is the cutting force expended in overcoming cutting resistance [7]. Equation (4) presents the energy consumption model P (Wh) representing the machine tool operating mode (positioning and acceleration of the spindle after a tool change/machining/returning of the spindle to tool exchange position after machining/stopping of the spindle).

$$P = P1 \times (T1 + T2) + P2 \times T2 + P3 \times T3. \tag{4}$$

In equation (4),

$P1$: stable energy consumption of the machine under operating conditions apart from the operating state

$T1$: cycle time (h) in nonoperating state

$T2$: cycle time (h) in cutting state

$P2$: energy consumed (W) by spindle and servo motors during cutting

$P3$: energy consumed (W) by positioning the work and by spindle acceleration/deceleration to the specified speed

$T3$: time (h) required for positioning the work and spindle acceleration [16, 20]

The energy consumption type in machining processes is defined as total energy consumption (SEC) and specific cutting energy consumption (SCEC) required for removing 1 cubic meter of the chip. Equations (5) and (6) give the specific energy consumption (SEC) and shear energy consumption (SCEC) required for chip removal [16, 20].

$$\text{SEC}\left(\frac{\text{J}}{\text{mm}^3}\right) = P\,\text{total (kW)/MMR}\left(\frac{\text{mm}^3}{s}\right), \tag{5}$$

$$\text{SCEC}\left(\frac{\text{J}}{\text{mm}^3}\right) = P\,\text{cutting}\,(W)/\text{MMR}\left(\frac{\text{mm}^3}{s}\right). \tag{6}$$

Surface roughness values of the aluminum alloy workpiece after machining were determined using the Mitutoyo Surftest SJ-210 measurement device. Surface roughness (Ra and Rz) measurements were carried out in accordance with the ISO 4287 standard. After the experiments, the surface was measured at the beginning, in the middle, and at the end of each sample and the arithmetic average was taken as the surface roughness value.

3. Results, Analysis, and Discussion

3.1. Experimental Results. The flow indices were measured and then the energy power conversion equations (equations (2)–(6) and the total energy consumption of the 6061 aluminum alloy during metal cutting were calculated (Tables 3 and 4).These values were calculated for both the spindle servo motor and the X-axis servo motor. The low SEC and P_{cutting} (kW) levels held great significance for electricity consumption in the tables.

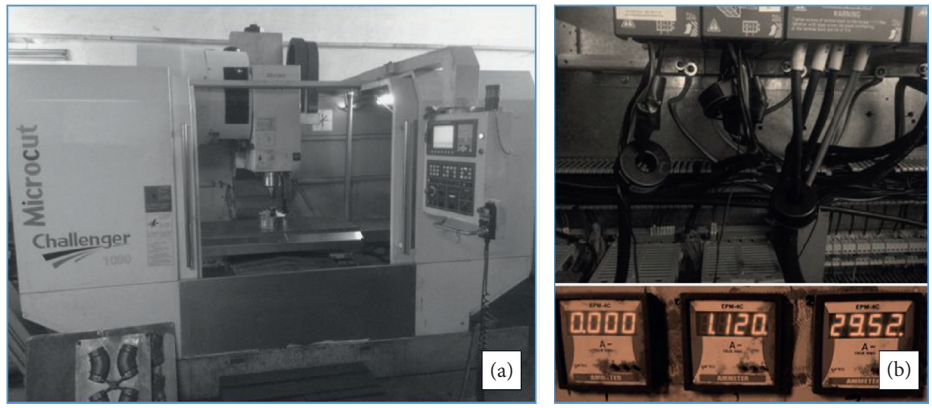

Figure 1: (a) Microcut 1000 CNC machining center. (b) Ammeter and current transformer drive connection.

Table 3: Experimental surface roughness results and *S*/*N* ratios.

Exp. no	*V* (m/min)	*f* (mm/rev)	DOC (mm)	Cm	*Ra* (μm)	*Ra*—*S*/*N* ratio (dB)	*Rz* (μm)	*Rz*—*S*/*N* ratio (dB)
1	60	0.10	0.5	1	1.120	−0.9844	7.2052	−17.1530
2	60	0.15	1.0	1	3.120	−9.8831	17.3440	−24.7830
3	60	0.20	1.5	2	5.460	−14.7439	31.0670	−29.8460
4	60	0.25	2.0	2	5.672	−15.0747	32.5755	−30.2578
5	120	0.10	1.0	2	2.540	−8.0967	27.4115	−28.7587
6	120	0.15	0.5	2	3.860	−11.7317	19.3407	−25.7294
7	120	0.20	2.0	1	3.120	−9.8831	23.8137	−27.5366
8	120	0.25	1.5	1	2.640	−8.4321	11.0873	−20.8965
9	180	0.10	1.5	1	1.650	−4.3497	9.3410	−19.4079
10	180	0.15	2.0	1	1.605	−4.1095	7.7330	−17.7670
11	180	0.20	0.5	2	1.580	−3.9731	9.4715	−19.5284
12	180	0.25	1.0	2	2.672	−8.5367	12.8927	−22.2069
13	240	0.10	2.0	2	2.832	−9.0419	15.8005	−23.9734
14	240	0.15	1.5	2	1.720	−4.7106	10.8800	−20.7326
15	240	0.20	1.0	1	1.498	−3.5102	8.1025	−18.1724
16	240	0.25	0.5	1	2.502	−7.9657	16.5083	−24.3541

Table 4: Experimental energy consumption results and *S*/*N* ratios.

Exp. no	*V* (m/min)	*F* (mm/rev)	DOC (mm)	Cm	$P_{cutting}$ *S* (W)	$P_{cutting}$ *S*—*S*/*N* ratio (dB)	SEC *S* (J)	SEC *S*—*S*/*N* ratio (dB)
1	60	0.10	0.5	1	7.89	−17.9402	242.80	−47.7051
2	60	0.15	1.0	1	15.78	−23.9608	81.43	−38.2161
3	60	0.20	1.5	2	118.33	−41.4620	41.96	−32.4574
4	60	0.25	2.0	2	23.67	−27.4826	24.33	−27.7230
5	120	0.10	1.0	2	457.55	−53.2088	37.39	−31.4558
6	120	0.15	0.5	2	173.55	−44.7887	44.21	−32.9098
7	120	0.20	2.0	1	1356.87	−62.6508	12.96	−22.2540
8	120	0.25	1.5	1	1135.99	−61.1075	12.90	−22.2094
9	180	0.10	1.5	1	1388.43	−62.8505	20.61	−26.2806
10	180	0.15	2.0	1	1735.54	−64.7887	11.52	−21.2310
11	180	0.20	0.5	2	694.21	−56.8299	23.43	−27.3965
12	180	0.25	1.0	2	1609.32	−64.1328	13.23	−22.4304
13	240	0.10	2.0	2	2295.64	−67.2181	17.01	−24.6160
14	240	0.15	1.5	2	2208.86	−66.8834	14.85	−23.4324
15	240	0.20	1.0	1	1672.43	−64.4669	14.65	−23.3141
16	240	0.25	0.5	1	883.55	−58.9246	18.50	−25.3420

Information about the workability of the product was also revealed by these data as the quality of the machining was directly affected by changes in the surface roughness.

Examination of the graphs in Figure 2 shows that the surface roughness values reached the highest levels in the first four experiments, especially in the 3rd and 4th experiments. In these two experiments, maximum surface roughness values were achieved under dry cutting conditions with increases in depth of cut and feed rate. Depending on different materials and processing parameters, other

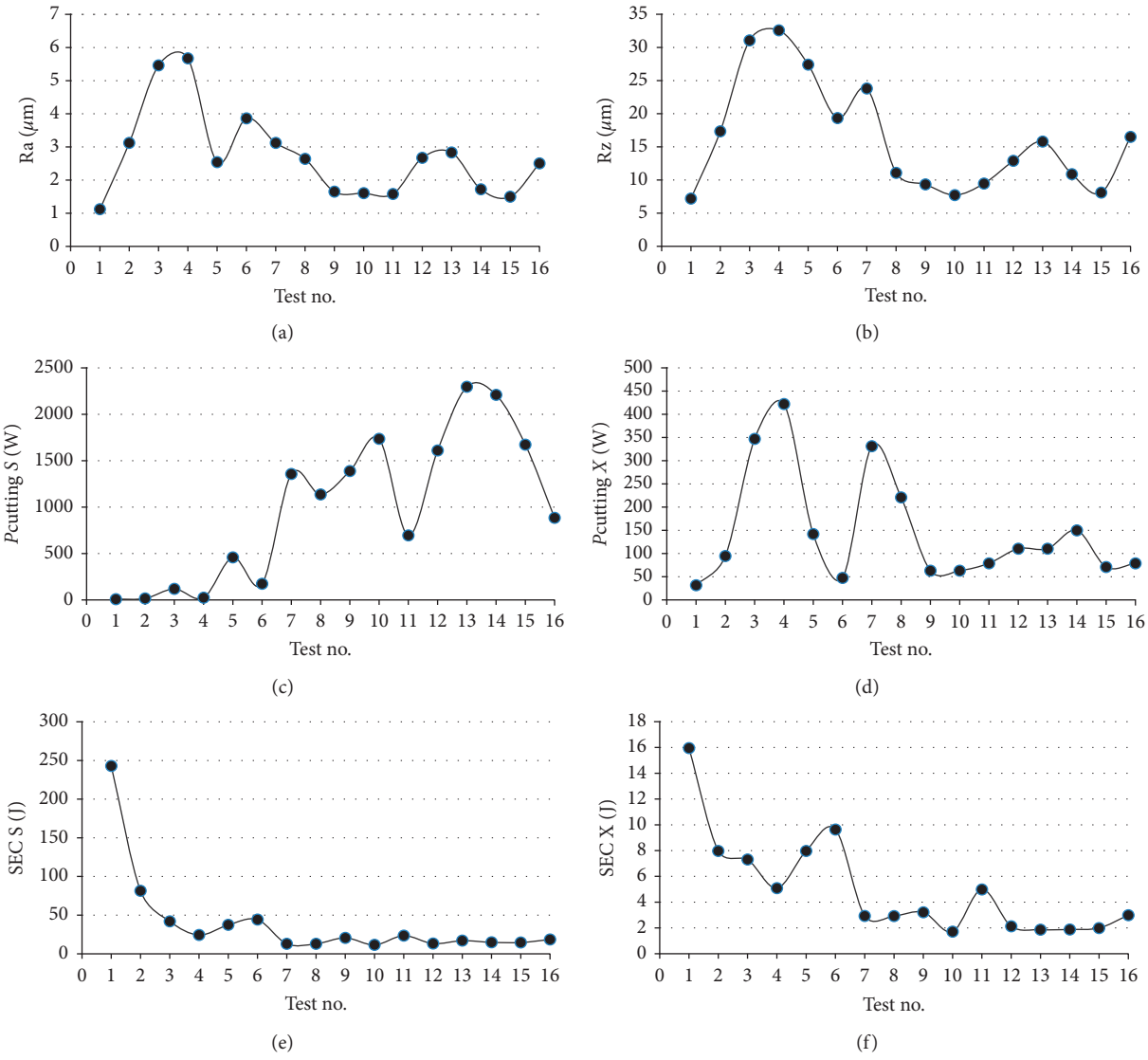

Figure 2: Experimental results for surface roughness and energy consumption.

studies have obtained similar results by applying dry cutting [13]. The SEC of both servo motors can be seen to occur in very high amounts at low revolutions. Similar results have been obtained in other studies [9, 13, 16]. A correlation can be seen between P_{cutting} change and surface roughness values. Such a result had not previously been included in the literature. In order to express this relationship in graphic form, Figure 3 presents the effects of P_{cutting} values of both spindle (S) and X-axis (X) servo motors on the surface roughness (Table 5).

When this figure is examined in detail, it has been determined that there may be a relationship between the P_{cutting} S value measured from the spindle engine and the amount of surface roughness. It can be said that this cutting power is generally high for low surface roughness. On the other hand, when the surface roughness was greater than 4, this P_{cutting} S value shows the lowest results for the spindle axis. Also, with an increase in the P_{cutting} X values of the X-axis servo motor, the amount of surface roughness stepped up in direct proportion. According to the results in this graph, the power of the X-axis servo motor has increased due to the probable ascend in the cutting force. At the same time, it is thought that the increase of these forces has stepped up the amount of surface roughness. The most likely reason for this situation was the BUE property of the 6061 alloy [21–24], which caused a reduction in its workability. Although a low surface roughness value was obtained during the ideal stock removal process, the stock removal energy consumption of the X-axis servo motor increased. The increase in X-axis motor energy consumption and reduction in the spindle servo motor energy consumption led to a general increase in the surface roughness value. These results demonstrated that the forces directly affected electricity consumption and surface roughness.

3.2. Optimization of Surface Roughness (Ra and Rz) and Energy Consumption (SEC S, $P_{cutting}$ S, SEC X, and $P_{cutting}$ X) Outputs. In the studies in the literature, different types of

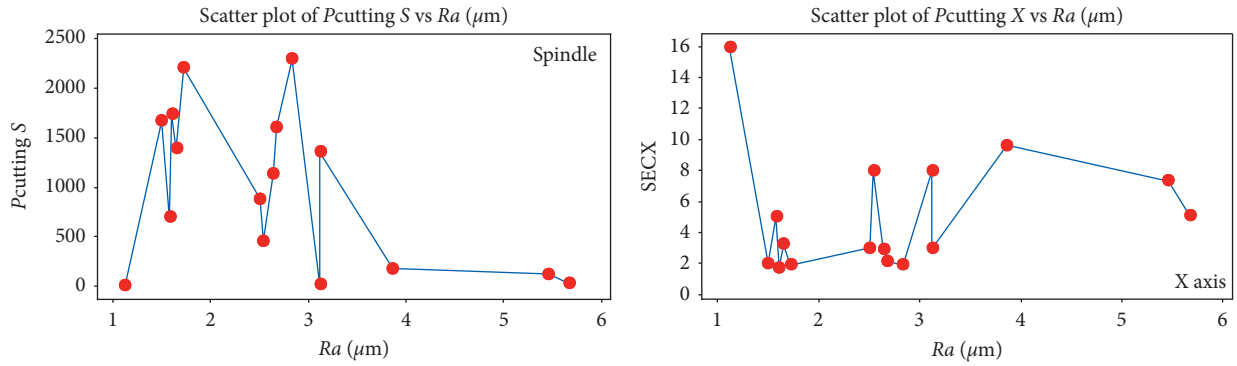

Figure 3: Scatter plots of $P_{cutting}$ S and $P_{cutting}$ X vs. Ra.

Table 5: Experimental energy consumption results and S/N ratios.

Exp. No	V (m/min)	f (mm/rev)	DOC (mm)	Cm	$P_{cutting}$ X (W)	$P_{cutting}$ X—S/N ratio (dB)	SEC X (J)	SEC X—S/N ratio (dB)
1	60	0.10	0.5	1	31.56	−29.9814	15.95	−24.0576
2	60	0.15	1.0	1	94.67	−39.5238	7.98	−18.0370
3	60	0.20	1.5	2	347.11	−50.8093	7.31	−17.2812
4	60	0.25	2.0	2	422.05	−52.5073	5.09	−14.1266
5	120	0.10	1.0	2	142.00	−43.0457	7.98	−18.0370
6	120	0.15	0.5	2	47.33	−33.5032	9.64	−19.6807
7	120	0.20	2.0	1	331.33	−50.4052	2.93	−9.3347
8	120	0.25	1.5	1	220.89	−46.8834	2.92	−9.3224
9	180	0.10	1.5	1	63.11	−36.0020	3.21	−10.1383
10	180	0.15	2.0	1	63.11	−36.0020	1.72	−4.6969
11	180	0.20	0.5	2	78.89	−37.9402	4.99	−13.9546
12	180	0.25	1.0	2	110.44	−40.8628	2.13	−6.5563
13	240	0.10	2.0	2	110.44	−40.8628	1.87	−5.4352
14	240	0.15	1.5	2	149.89	−43.5153	1.88	−5.4993
15	240	0.20	1.0	1	71.00	−37.0251	1.99	−5.9958
16	240	0.25	0.5	1	78.89	−37.9402	2.99	−9.5176

coolants and machining processes, variable cutting parameters, the Taguchi experimental design, and ANOVA analyses have been used to investigate surface roughness. Previous studies have accounted for the spindle motor energy consumed during the cutting process dependent on the cutting speed. In this study, the energy consumption values of both spindle servo motor and X-axis servo motor were calculated and compared with the surface roughness results. In this way, energy expenditure on the X-axis motor, which determines the feed rate, was measured and the effects on surface roughness were investigated. In the slot milling operation, the influence of the BUE of the A6061 was determined under dry and coolant fluid cutting conditions. The Taguchi L_{16} orthogonal array was used to carry out machining tests on Al T6061 alloy. The optimum levels of cutting speed, feed rate, and depth of cut were determined for energy consumption and surface roughness, and these values were used in the calculation of the S/N ratios (Tables 3–5).

The Taguchi method was used to generate the S/N responses which were used in the determination of the control factors most effective on the optimal levels of surface roughness and energy consumption. In this table, the highest S/N values represent the optimal levels of each control factor. Table 6 gives the effect of each control factor on surface roughness and energy consumption as shown by the S/N responses. The values in this table are obtained as a result of Taguchi optimization. We can determine the most effective input parameters on the output parameters and values in this table. However, the order of effects between the parameters is also determined. The response table is similar to analysis of variance. But rarely, it may differ. ANOVA results showed a parallel with the S/N response table in this study. The cutting speed, feed rate, depth of cut, and cooling method, respectively, were found to be the most effective factors on the surface roughness and energy consumption. The ANOVA results confirmed these findings.

The main effect graph in Figure 4 shows the optimum values for the control factors (machining parameters). As in the S/N response table, the optimum level is indicated by the highest S/N value for each parameter in this graph. The optimal cutting speed, feed rate, depth of cut, and cooling method values determined for Ra were, respectively, 180 m/min, 0.10 mm/rev, 0.5 mm, and wet machining, and for Rz, they were, respectively, 180 m/min, 0.15 mm/rev, 0.5 mm, and wet machining. The optimal values determined for

Table 6: *S/N* response table for surface roughness and energy consumption.

	Level	V (m/min)	f (mm/rev)	DOC (mm)	Cm
Ra (μm)	1	−10.172	**−5.618**	**−6.164**	**−6.140**
	2	−9.536	−7.609	−7.507	−9.489
	3	**−5.242**	−8.028	−8.059	
	4	−6.307	−10.002	−9.527	
	Delta	4.929	4.384	3.364	
	Rank	1	2	3	4
Rz (μm)	1	−25.51	−22.32	**−21.69**	**−21.26**
	2	−25.73	**−22.25**	−23.48	−25.13
	3	**−19.73**	−23.77	−22.72	
	4	−21.81	−24.43	−24.88	
	Delta	6.00	2.18	3.19	3.87
	Rank	1	4	3	2
P_{cutting} S (W)	1	**−27.71**	−50.30	**−44.62**	**−52.09**
	2	−55.44	**−50.11**	−51.44	−52.75
	3	−62.15	−56.35	−58.08	
	4	−64.37	−52.91	−55.54	
	Delta	36.66	6.25	13.46	0.66
	Rank	1	3	2	4
P_{cutting} X (W)	1	−43.21	**−37.47**	**−34.84**	**−39.22**
	2	−43.46	−38.14	−40.11	−42.88
	3	**−37.70**	−44.04	−44.30	
	4	−39.84	−44.55	−44.94	
	Delta	5.76	7.08	10.10	3.66
	Rank	3	2	1	4
SEC S (J)	1	−36.53	−32.51	−33.34	−28.32
	2	−27.21	−28.95	−28.85	**−27.80**
	3	−24.33	−26.36	−26.09	
	4	**−24.18**	**−24.43**	**−23.96**	
	Delta	12.35	8.09	9.38	0.52
	Rank	1	3	2	4
SEC X (J)	1	−18.376	−14.417	−16.803	**−11.388**
	2	−14.094	−11.978	−12.157	−12.571
	3	−8.837	−11.642	−10.560	
	4	**−6.612**	**−9.881**	**−8.398**	
	Delta	11.764	4.536	8.404	1.184
	Rank	1	3	2	4

$P_{\text{cutting}}S$ were 60 m/min, 0.15 mm/rev, 0.5 mm, and wet machining, and for $P_{\text{cutting}}X$, they were 180 m/min, 0.10 mm/rev, 0.5 mm, and wet machining. For SEC S, these values were 240 m/min, 0.25 mm/rev, 2.0 mm, and dry machining, and for SEC X, they were 240 m/min, 0.25 mm/rev, 2.0 mm, and wet machining.

3.3. Variance Analyses (ANOVA). Table 7 presents the results of the ANOVA (95% CI and 5% significance level) for the control factor effect levels on surface roughness and energy consumption. The table shows the F values and the percentage contribution ratio (PCR) with the significance level of each variable. The F values, as the factors having the most influence on the results, were compared in order to determine the effect of the control factors.

The ANOVA results revealed the cutting speed (36.18%) to be the most important parameter affecting *Ra*, followed by the cooling method (19.32%) and feed rate (14.26), with the depth of cut effective on *Ra* at low levels (9.62%). The parameters found most effective on *Rz* were cutting speed (39.07%), cooling method (20.04%), depth of cut (9.10%), and feed rate (5.71%). On P_{cutting} S, the most effective parameters were cutting speed (70.20%), depth of cut (20.35%), feed rate (0.45%), and cooling method (0.25%), while on P_{cutting} X, they were depth of cut (35.73%), feed rate (26.97%), cutting speed (26.28%), and cooling method (6.04%). The parameters most effective on SEC S were cutting speed (37.34%), depth of cut (21.63%), feed rate (19.24%), and cooling method (5.05%), and on SEC X, these were cutting speed (51.40%), depth of cut (30.31%), feed rate (15.09%), and cooling method (0.04%). The ANOVA results verified the *S/N* response results (Table 6) and the findings of the main effect graphs (Figure 4).

3.4. Confirmation Tests. The experimental study obtained optimum surface roughness and energy consumption results via application of the Taguchi optimization method. The ANOVA results revealed the effective percentage distributions of the parameters. As a final step, the validity of the optimization process was assessed by confirmation experiments. The Taguchi method was used to determine and calculate surface roughness and energy consumption values by applying equations (7)–(18) [25–27]. Using these equations under optimal milling conditions, *Ra*, *Rz*, P_{cutting} S, P_{cutting} X, SEC S, and SEC X were calculated, respectively, as 0.968 μm, 5.853 μm, 7.306 W, 20.133 W, 6.447 J, and 1.039 J.

$$\begin{aligned}\text{Ra} - \eta_G = {} & \overline{\eta}_G + (\overline{A}_3 - \overline{\eta}_G) + (\overline{B}_1 - \overline{\eta}_G) \\ & + (\overline{C}_1 - \overline{\eta}_G) + (\overline{D}_1 - \overline{\eta}_G),\end{aligned} \tag{7}$$

$$Ra_{\text{cal}} = 10^{-\eta_G/20}, \tag{8}$$

$$\begin{aligned}\text{Rz} - \eta_G = {} & \overline{\eta}_G + (\overline{A}_3 - \overline{\eta}_G) + (\overline{B}_2 - \overline{\eta}_G) \\ & + (\overline{C}_1 - \overline{\eta}_G) + (\overline{D}_1 - \overline{\eta}_G).\end{aligned} \tag{9}$$

$$Rz_{\text{cal}} = 10^{-\eta_G/20}, \tag{10}$$

$$\begin{aligned}P_{\text{cutting}}S - \eta_G = {} & \overline{\eta}_G + (\overline{A}_1 - \overline{\eta}_G) + (\overline{B}_2 - \overline{\eta}_G) \\ & + (\overline{C}_1 - \overline{\eta}_G) + (\overline{D}_1 - \overline{\eta}_G).\end{aligned} \tag{11}$$

$$P_{\text{cutting}}S_{\text{cal}} = 10^{-\eta_G/20}, \tag{12}$$

$$\begin{aligned}P_{\text{cutting}}X - \eta_G = {} & \overline{\eta}_G + (\overline{A}_3 - \overline{\eta}_G) + (\overline{B}_1 - \overline{\eta}_G) \\ & + (\overline{C}_1 - \overline{\eta}_G) + (\overline{D}_1 - \overline{\eta}_G).\end{aligned} \tag{13}$$

$$P_{\text{cutting}}X_{\text{cal}} = 10^{-\eta_G/20}, \tag{14}$$

$$\begin{aligned}\text{SEC}\,S - \eta_G = {} & \overline{\eta}_G + (\overline{A}_4 - \overline{\eta}_G) + (\overline{B}_4 - \overline{\eta}_G) \\ & + (\overline{C}_4 - \overline{\eta}_G) + (\overline{D}_2 - \overline{\eta}_G),\end{aligned} \tag{15}$$

$$\text{SEC}\,S_{\text{cal}} = 10^{-\eta_G/20}, \tag{16}$$

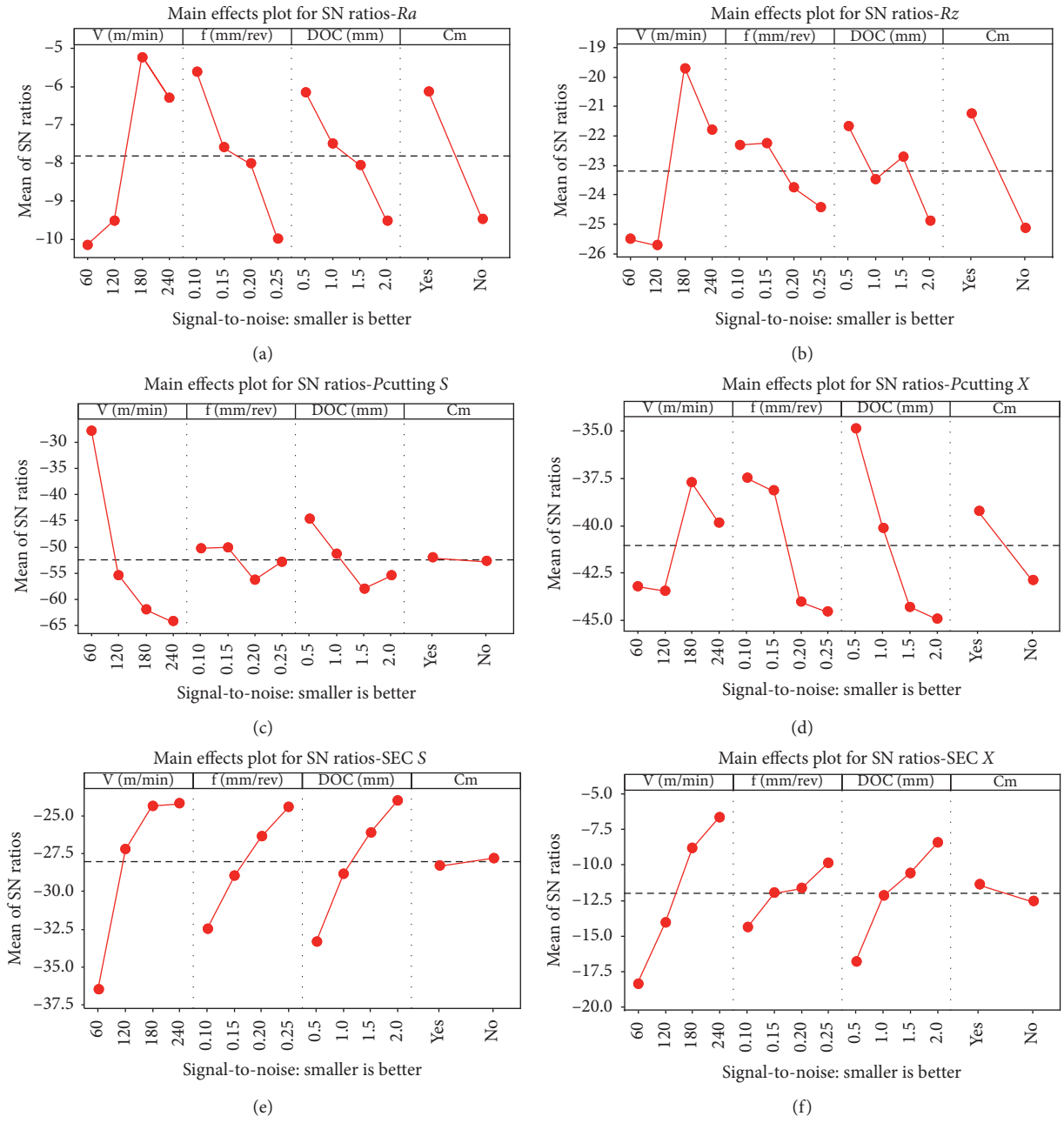

Figure 4: Main effect plot of *S*/*N* ratios.

$$\text{SEC } X - \eta_G = \overline{\eta}_G + (\overline{A}_4 - \overline{\eta}_G) + (\overline{B}_4 - \overline{\eta}_G) + (\overline{C}_4 - \overline{\eta}_G) + (\overline{D}_1 - \overline{\eta}_G), \quad (17)$$

$$\text{SEC } X_{\text{cal}} = 10^{-\eta_G/20}. \quad (18)$$

In equations (7)–(18),

$\boldsymbol{\eta}_G$: *S*/*N* ratio calculated for the optimum levels

$\overline{\boldsymbol{\eta}}_G$: average *S*/*N* ratio for all variables

$\overline{\mathbf{A}}_{1-4}$: optimum *S*/*N* ratio for factor A

$\overline{\mathbf{B}}_{1-4}$: optimum *S*/*N* ratio for factor B

$\overline{\mathbf{C}}_{1-4}$: optimum *S*/*N* ratio for factor C

$\overline{\mathbf{D}}_{1-4}$: optimum *S*/*N* ratio for factor D

*Ra*cal, *Rz*cal, P_{cutting} *S*cal, P_{cutting} *X*cal, SEC *S*cal, and SEC *X*cal: the calculated surface roughness and energy consumption values for the optimum level.

$$CI_{Ra,Rz,P_{\text{cutting}}S,P_{\text{cutting}}X,\text{SEC }S,\text{SEC }X} = \sqrt{F_{\alpha,1,f_e}.V_e\left[\frac{1}{n_{\text{eff}}}+\frac{1}{R}\right]}, \quad (19)$$

where $F_{\alpha,1,f_e}$: F ratio at 95% CI, α: level of significance, f_e: degrees of freedom of error, V_e: error variance, n_{eff}: effective number of replications, and *R*: number of confirmation experiment replications.

Table 7: ANOVA results.

Source	Degree of freedom (DF)	Sum of squares (SS)	Mean square (MS)	F ratio	P	PCR (%)
Ra						
V	3	9.653	3.2177	2.92	0.139	36.18
F	3	3.806	1.2685	1.15	0.414	14.26
DOC	3	2.568	0.8560	0.78	0.555	9.62
Cm	1	5.154	5.1540	4.68	0.083	19.32
Error	5	5.503	1.1005			20.62
Total	15	26.683				100.00
Rz						
V	3	414.11	138.04	2.50	0.174	39.07
F	3	60.53	20.18	0.36	0.782	5.71
DOC	3	96.42	32.14	0.58	0.653	9.10
Cm	1	212.46	212.46	3.84	0.107	20.04
Error	5	276.50	55.30			26.08
Total	15	1060.02				100.00
P_{cutting} *S*						
V	3	6715363	2238454	13.38	0.008	70.20
F	3	43408	14469	0.09	0.964	0.45
DOC	3	1946747	648916	3.88	0.089	20.35
Cm	1	23664	23664	0.14	0.722	0.25
Error	5	836803	167361			8.75
Total	15	9565984				100.00
P_{cutting} *X*						
V	3	55966	18655	8.79	0.019	26.28
F	3	57429		9.02	0.018	26.97
DOC	3	76099	25366	11.96	0.010	35.73
Cm	1	12860	12860	6.06	0.057	6.04
Error	5	10608	2122			4.98
Total	15	212961				100.00
SEC *S*						
V	3	18308	6103	3.72	0.096	37.34
F	3	9433	3144	1.92	0.245	19.24
DOC	3	10606	3535	2.15	0.212	21.63
Cm	1	2474	2474	1.51	0.274	5.05
Error	5	8205	1641			16.74
Total	15	49026				100.00
SEC *X*						
V	3	117.182	39.0605	27.07	0.002	51.40
F	3	34.395	11.4651	7.95	0.024	15.09
DOC	3	69.097	23.0323	15.96	0.005	30.31
Cm	1	0.087	0.087	0.0868	0.816	0.04
Error	5	7.214	1.4429			3.16
Total	15	227.975				100.00

$$n_{\text{eff}} = \frac{N}{1 + T_{\text{dof}}}. \tag{20}$$

In equation (20), N: total number of experiments, T_{dof}: total main factor degrees of freedom.

$F_{0.05,\ 1,\ 5} = 6.608$ (from F test table), $V_{eRa,} = 1.1005$, $V_{eRz} = 55.30$, $V_{eP\ \text{cutting}\ S} = 167361$, $V_{eP\ \text{Cutting}\ X} = 2122$, $V_{\text{eSEC}\ S} = 1641$, $V_{\text{eSEC}\ X} = 114429$ (Table 7), and $R = 3$ (equation (19)).

$N = 16$, $T_{\text{dof}} = 10$, and $n_{\text{eff}} = 1.454$ (equation (20)).

By using equations (19) and (20), the CI were calculated as CI_{Ra}, CI_{Rz}, $\text{CI}_{P\text{cutting}\ S}$, $\text{CI}_{P\ \text{cutting}\ X}$, $\text{CI}_{\text{SEC}\ S}$, and $\text{CI}_{\text{SEC}\ X}$, respectively = ± 2.724, ±19.315, 1062.607, 119.651, 105.220, and 878.645. The average optimal *Ra*, *Rz*, P_{cutting} *S*, P_{cutting} *X*, SEC *S*, and SEC *X* (CI 95%) were:

$(Ra_{\text{opt}} - \text{CI}_{Ra}) < Ra_{\text{exp}} < (Ra_{\text{opt}} + \text{CI}_{Ra}) = (0.968–2.724) < 1.042 < (0.968 + 2.724) = -1.756 < 1.042 < 3.692.$

$(Rz_{\text{opt}} - \text{CI}_{Rz}) < Rz_{\text{exp}} < (Rz_{\text{opt}} + \text{CI}_{Rz}) = (5.853–19.315) < 6.726 < (5.853 + 19.315) = -13.732 < 6.726 < 25.168.$

$(P_{\text{cutting}}\ S_{\text{opt}} - \text{CI}_{P\ \text{cutting}\ S}) < P_{\text{cutting}}\ S_{\text{exp}} < (P_{\text{cutting}}\ S_{\text{opt}} + \text{CI}_{P\ \text{cutting}\ S}) = (7.306–1062.607) < 7.108 < (7.306 + 1062.607) = -1055.301 < 7.108 < 1069.913.$

$(P_{\text{cutting}}\ X_{\text{opt}} - \text{CI}_{P\ \text{Cutting}\ X}) < P_{\text{cutting}}\ X_{\text{exp}} < (P_{\text{cutting}}\ X_{\text{opt}} + \text{CI}_{P\ \text{cutting}\ X}) = (20.133–119.651) < 23.643 < (20.133 + 119.651) = -99.518 < 23.643 < 139.784.$

Table 8: Confirmation test results for predicted and experimental values.

Optimum levels	Parameters	Exp.	Pred.	Error (%)
$A_3B_1C_1$ D_1	*Ra*	1.042	0.968	7.10
$A_3B_2C_1$ D_1	*Rz*	6.726	5.853	12.97
$A_1B_2C_1$ D_1	$P_{cutting}$ *S*	7.108	7.306	2.78
$A_3B_1C_1$ D_1	$P_{cutting}$ *X*	23.643	20.133	14.84
$A_4B_4C_4$ D_2	SEC *S*	7.554	6.447	14.65
$A_4B_4C_4$ D_1	SEC *X*	1.203	1.039	13.63

$$(\text{SEC } S_{opt} - \text{CI}_{\text{SEC } S}) < \text{SEC } S_{exp} < (\text{SEC } S_{opt} + \text{CI}_{\text{SEC } S}) = (6.447 - 105.220) < 7.545 < (6.447 + 105.220) = -98.773 < 7.545 < 111.667.$$

$$(\text{SEC } X_{opt} - \text{CI}_{\text{SEC } X}) < \text{SEC } X_{exp} < (\text{SEC } X_{opt} + \text{CI}_{\text{SEC } X}) = (1.039 - 878.645) < 1.203 < (1.039 + 878.645) = -877.606 < 1.203 < 879.684.$$

The experimental values of Ra_{exp}, Rz_{exp}, P_{Cutting} S_{exp}, $P_{cutting}$ X_{exp}, SEC S_{exp}, and SEC X_{exp} were found to be within acceptable CI limits. Thus, the Taguchi method had successfully optimized the surface roughness and energy consumption values ($p = 0.05$). This success was reflected in the results of the confirmation experiments. The Taguchi method was used to perform confirmation tests at optimum levels for the control factors. A comparison of the experimental test results with the Taguchi method predicted values is shown in Table 8. The predicted values and the experimental values can be seen to be very close. In order for statistical analyses to be considered reliable, error values must be below 20% [28, 29]. Many important studies have been carried out on energy consumption during the machining process [30–33]. The comparison of surface roughness and energy consumption values (Table 8) underscores the fact that the level of difference between the results of the confirmation test and those obtained via the Taguchi method was insignificant. Consequently, the successful optimization was reflected in the results of the confirmation tests.

4. Conclusions

For this study, in the slot milling of Al T6061 alloy, a number of milling experiments were performed and experimental and statistical analyses on energy consumption and surface roughness were carried out. The experiments were designed according to the Taguchi L_{16} orthogonal array and reached optimal surface roughness (*Ra* and *Rz*) and energy consumption ($P_{cutting}$ *S*, $P_{cutting}$ *X*, SEC *S*, and SEC *X*) values in a shorter time with 16 experiments instead of 128, resulting in savings of time and cost. This study determined the energy consumption of both servo motors used in the processing of the 6061 alloy, which is widely used in industry but has low workability due to BUE. Furthermore, the effects of these energy consumption values on the surface roughness values were also determined. The cutting parameters effective on energy consumption and surface roughness were determined via ANOVA. Confirmation experiments were conducted to assess the validity of the optimization. In conclusion, the following results were obtained from the study:

(i) The surface roughness decreased as the energy consumption value increased for the spindle axis motor during cutting.

(ii) On the contrary, as energy consumption values of the *X*-axis servo motor increased during cutting, the amount of surface roughness increased in direct proportion.

(iii) The optimal *Ra* values for the cutting speed, feed rate, depth of cut, and cooling method were determined as 180 m/min, 0.10 mm/rev, 0.5 mm, and wet machining, respectively, whereas the optimal values for *Rz* were 180 m/min, 0.15 mm/rev, 0.5 mm, and wet machining.

(iv) The optimal $P_{cutting}$ *S* values for the cutting speed, feed rate, depth of cut, and cooling method were determined as 60 m/min, 0.15 mm/rev, 0.5 mm, and wet machining, respectively, whereas the optimal values for $P_{cutting}$ *X* were 180 m/min, 0.10 mm/rev, 0.5 mm, and wet machining.

(v) The optimal SEC *S* values for the cutting speed, feed rate, depth of cut, and cooling method were determined as 240 m/min, 0.25 mm/rev, 2.0 mm, and dry machining, respectively, while the optimum values for SEC *X* were 240 m/min, 0.25 mm/rev, 2.0 mm, and wet machining.

(vi) The ANOVA results determined the most important parameter effective on *Ra* and *Rz* to be the cutting speed, at 36.18% and 39.07%, respectively.

(vii) The parameter most effective on $P_{cutting}$ *S* was determined as the cutting speed (70.20%), whereas for $P_{cutting}X$, it was depth of cut (35.73%).

(viii) The most effective parameter on SEC *S* and SEC *X* was the cutting speed, at 37.34% and 51.40%, respectively.

(ix) According to the confirmation test, the values measured were found to be within the 95% confidence interval (CI).

As demonstrated by the optimization results, the Taguchi experimental design method was shown to have been successfully applied in the determination of the optimal values for surface roughness and energy consumption in the slot milling of the Al T6061 alloy.

Nomenclature

A: Power indices
ANOVA: Analysis of variance
BU: Built up edge
CI: Confidence interval
Cm: Cooling method
CNC: Computer numerical control
DOC: Depth of cut
DF: Degree of freedom
EC: Energy consumption

f: Feed rate
f_e: Degrees of freedom of error
h: Cycle time
MS: Mean square
N: Noise factor
n_{eff}: Effective number of replications
PCR: Percentage contribution ratio
PI: Power index (A)
PVD: Physical vapor deposition
P_{air}: Energy consumption when the machine does not remove chips
P_{idle}: Energy consumption when the machine does not remove chips
P_{total}: Total power consumption
P_{cutting}: The energy consumption during cutting
P_{cutting} S: Power consumption in the S-axis
P_{cutting} X: Power consumption in the X-axis
R: Number of confirmation experiment replications
Ra: Surface roughness
S: Signal factor
SS: Sum of squares
SEC: Specific energy consumption
SCEC: Specific cutting energy consumption
SEC S: Specific energy consumption in the S-axis
SEC X: Specific energy consumption in the X-axis
T_{dof}: Total main factor degrees of freedom
V: Cutting speed
v: Voltage
V_e: Error variance.

Data Availability

The data used to support the findings of this study are available from the corresponding author upon request.

Conflicts of Interest

The authors declare that they have no conflicts of interest.

References

[1] H. Quan, Y. Chai, R. Li, G.-Y. Peng, and Y. Guo, "Influence of circulating-flow's geometric characters on energy transition of a vortex pump," *Engineering Computations*, vol. 36, no. 9, pp. 3122–3137, 2019.

[2] S. Liu, X. Ding, and Z. Tong, "Energy absorption properties of thin-walled square tube with lateral piecewise variable thickness under axial crashing," *Engineering Computations*, vol. 36, no. 8, pp. 2588–2611, 2019.

[3] B. Öztürk, "Energy consumption model for the pipe threading process using 10 wt.-% Cu and 316L stainless steel powder-reinforced aluminum 6061 fittings," *Materials Testing*, vol. 61, no. 8, pp. 797–805, 2019.

[4] H. Demir and S. Gündüz, "The effects of aging on machinability of 6061 aluminium alloy," *Materials & Design*, vol. 30, no. 5, pp. 1480–1483, 2009.

[5] E. Nas and H. Gökkaya, "Experimental and statistical study on machinability of the composite materials with metal matrix Al/B4c/graphite," *Metallurgical and Materials Transactions A*, vol. 48, no. 10, pp. 5059–5067, 2017.

[6] M. S. Sukumar, P. V. Ramaiah, and A. Nagarjuna, "Optimization and prediction of parameters in face milling of Al-6061 using Taguchi and ANN approach," *Procedia Engineering*, vol. 97, pp. 365–371, 2014.

[7] M. Mori, M. Fujishima, Y. Inamasu, and Y. Oda, "A study on energy efficiency improvement for machine tools," *CIRP Annals*, vol. 60, no. 1, pp. 145–148, 2011.

[8] N. Liu, Y. F. Zhang, and W. F. Lu, "A hybrid approach to energy consumption modelling based on cutting power: a milling case," *Journal of Cleaner Production*, vol. 104, pp. 264–272, 2015.

[9] C. Camposeco-Negrete, "Optimization of cutting parameters for minimizing energy consumption in turning of AISI 6061 T6 using Taguchi methodology and ANOVA," *Journal of Cleaner Production*, vol. 53, pp. 195–203, 2013.

[10] Y. Oda, M. Mori, K. Ogawa, S. Nishida, M. Fujishima, and T. Kawamura, "Study of optimal cutting condition for energy efficiency improvement in ball end milling with tool-workpiece inclination," *CIRP Annals*, vol. 61, no. 1, pp. 119–122, 2012.

[11] Y. Shokoohi, E. Khosrojerdi, and B. H. Rassolian Shiadhi, "Machining and ecological effects of a new developed cutting fluid in combination with different cooling techniques on turning operation," *Journal of Cleaner Production*, vol. 94, pp. 330–339, 2015.

[12] R. Neugebauer, A. Schubert, B. Reichmann, and M. Dix, "Influence exerted by tool properties on the energy efficiency during drilling and turning operations," *CIRP Journal of Manufacturing Science and Technology*, vol. 4, no. 2, pp. 161–169, 2011.

[13] P. Muñoz-Escalona, A. Shokrani, and S. T. Newman, "Influence of cutting environments on surface integrity and power consumption of austenitic stainless steel," *Robotics and Computer-Integrated Manufacturing*, vol. 36, pp. 60–69, 2015.

[14] E. Nas and B. Öztürk, "Optimization of surface roughness via the Taguchi method and investigation of energy consumption when milling spheroidal graphite cast iron materials," *Materials Testing*, vol. 60, no. 5, pp. 519–525, 2018.

[15] X. Zhou, F. Liu, and W. Cai, "An energy-consumption model for establishing energy-consumption allowance of a workpiece in a machining system," *Journal of Cleaner Production*, vol. 135, pp. 1580–1590, 2016.

[16] N. Liu, S. B. Wang, Y. F. Zhang, and W. F. Lu, "A novel approach to predicting surface roughness based on specific cutting energy consumption when slot milling Al-7075," *International Journal of Mechanical Sciences*, vol. 118, pp. 13–20, 2016.

[17] S. Sarkar, A. Bhirangi, J. Mathew, R. Oyyaravelu, P. P. Kuppan, and A. S. S. Balan, "Fabrication characteristics and mechanical behavior of rice husk ash-silicon carbide reinforced Al-6061 alloy matrix hybrid composite," *Materials Today: Proceedings*, vol. 5, no. 5, pp. 12706–12718, 2018.

[18] B. Öztürk and F. Erzincanli, "Development of femoral component design geometry by using DMROVAS (design method requiring optimum volume and safety)," *Engineering Computations*, vol. 37, no. 2, pp. 682–704, 2019.

[19] M. Karabatak and F. Kara, "Experimental optimization of surface roughness in hard turning of AISI D2 cold work tool steel," *Journal of Polytechnic*, vol. 19, no. 3, pp. 349–355, 2016.

[20] M. Mia, G. Singh, M. K. Gupta, and V. S. Sharma, "Influence of Ranque-Hilsch vortex tube and nitrogen gas assisted MQL in precision turning of Al 6061-T6," *Precision Engineering*, vol. 53, pp. 288–299, 2018.

[21] F. Klocke, G. Eisenblätter, and T. Krieg, "Machining: wear of tools," in *Encyclopedia of Materials: Science and Technology*, pp. 4708–4711, Elsevier, Oxford, UK, 2008.
[22] N. Masmiati, H. S. Chan, A. A. D. Sarhan, M. A. Hassan, and M. Hamdi, "Investigating the Possibility to reduce the residual stress level in 2.5D cutting using titanium coated carbide ball end mill," *Advances in Materials Science and Engineering*, vol. 2014, Article ID 485267, 13 pages, 2014.
[23] E. M. Trent and P. K. Wright, *Metal Cutting*, Butterworth-Heinemann, New York, NY, USA, 4th edition, 2000.
[24] M. Álvarez, J. Salguero, J. A. Sánchez, M. Huerta, and M. Marcos, "SEM and EDS characterisation of layering TiOxGrowth onto the cutting tool surface in hard drilling processes of Ti-Al-V alloys," *Advances in Materials Science and Engineering*, vol. 2011, Article ID 414868, 10 pages, 2011.
[25] F. Kara, "Taguchi optimization of surface roughness and flank wear during the turning of DIN 1.2344 tool steel," *Materials Testing*, vol. 59, no. 10, pp. 903–908, 2017.
[26] E. Yücel and H. Saruhan, "Design optimization of rotor-bearing system considering critical speed using Taguchi method," *Proceedings of the Institution of Mechanical Engineers, Part E: Journal of Process Mechanical Engineering*, vol. 231, no. 2, pp. 138–146, 2017.
[27] F. Kara, "Optimization of surface roughness in finish milling of AISI P20+S plastic-mold steel," *Materiali in Tehnologije*, vol. 52, no. 2, pp. 195–200, 2018.
[28] P. J. Ross, *Taguchi Techniques for Quality Engineering*, McGraw-Hill, New York, NY, USA, 1996.
[29] W. Li and S. Kara, "An empirical model for predicting energy consumption of manufacturing processes: a case of turning process," *Proceedings of the Institution of Mechanical Engineers, Part B: Journal of Engineering Manufacture*, vol. 225, no. 9, pp. 1636–1646, 2011.
[30] B. Öztürk, "Experimental research of energy consumption of austenitizing heat-treated casting fittings in pipe threading," *Sakarya University Journal of Science*, vol. 23, no. 5, pp. 869–878, 2019.
[31] B. Öztürk, L. Uğur, and A. Yildiz, "Investigation of effect on energy consumption of surface roughness in X-axis and spindle servo motors in slot milling operation," *Measurement*, vol. 139, pp. 92–102, 2019.
[32] K. Cheng, Ed., *Machining Dynamics: Teory, Applications and Practices*, Springer, London, UK, 2008.
[33] H. Ding, D. Guo, K. Cheng, and Q. Cui, "An investigation on quantitative analysis of energy consumption and carbon footprint in the grinding process," *Proceedings of the Institution of Mechanical Engineers, Part B: Journal of Engineering Manufacture*, vol. 228, no. 6, pp. 950–956, 2014.